Responses of Base-Isolated Buildings in Tokyo during the 2011 Great East Japan Earthquake

K. MATSUDA & K. KASAI
Tokyo Institute of Technology, Japan

H. YAMAGIWA
Okumura Corporation, Japan

D. SATO
Tokyo University of Science, Japan

SUMMARY:
Many buildings in the Tohoku and Kanto area were strongly shaken during the Great East Japan Earthquake, March 11, 2011. These results are precious data, since the response-control technologies are relatively new and very few systems have been validated through actual earthquakes, there has been some desire to determine their true capabilities. In this paper, recorded and examined results of base-isolated building are discussed. In particular, dynamic properties of a high-rise base-isolated building are focused. Modal properties of vibration period, damping ratio, and participation vectors are identified, by using the linear and nonlinear system identification techniques. The responses are compared with the hypothetical case that the superstructure had been fixed to the ground, and benefit of base-isolation is clearly demonstrated.

Keywords: Response Records, Base-Isolation, High-Rise Building, Steel Damper, System Identification

1. INTRODUCTION

At 14:46 on March 11, 2011, the East Japan Earthquake of magnitude 9.0 occurred off the Sanriku coast of Japan. The earthquake has a recorded seismic intensity of 7 in northern Miyagi prefecture, which is the highest intensity on the Japan Meteorological Agency scale. The East Japan Earthquake exemplifies how effective seismic protection technologies are at preventing earthquake damage, such as seismic base isolation and supplemental damping, have been increasingly used in Japan since the 1995 Great Hanshin Earthquake, with a hope to better protect not only human lives but also building functionality and assets.

The response records of the buildings should be collected. Since the response-control technologies are new and have not often been validated through response to actual earthquakes, there have been some desires to find their true capabilities. The collected records and examination also should be released to be useful for design method. In this paper, recorded and examined results of base-isolated building are discussed. In particular, dynamic properties of a high-rise base-isolated building such as vibration period and damping ratio are focused.

2. RESPONSE TRENDS OF BASE-ISOLATED BUILDINGS IN TOKYO AREA

Soon after the 2011 Great East Japan Earthquake, Japan Society of Seismic Isolation (JSSI) established the Response-Controlled Buildings Investigation Committee to set policies and action plans for detailed investigations into the actual performance of buildings that are base-isolated or supplementally-damped. The final reports of the committee were presented in the workshops held by JSSI in January 2012, and the final report documents are available (JSSI 2012). There are 20 base-isolated buildings in the report. The buildings also range from 2 stories to 21 stories, and about 60% of the buildings use natural rubber bearings with dampers, which is consistent with the

nationwide trend in Japan. Note also that about 40% of the buildings use high damping rubber bearing or lead rubber bearing, without utilizing externally attached dampers. Because of the wide geographical area, the peak ground acceleration (PGA) varies from 44.5 to 402 gal, and building top accelerations from 57 to 344 gal. The maximum displacement at the isolation level, typically estimated from the accelerations and their double integrations, ranged from 2.9 to 18.0 cm.

As shown in Figure 1, the building top acceleration normalized to the PGA, hereby referred to as the acceleration magnification ratio (AMR), is estimated for each horizontal direction and each building, and it is plotted against the PGA (Kasai et al.). Remarkably, AMR and PGA are strongly correlated, and AMR becomes smaller for the larger PGA. The hysteretic characteristic of the base-isolated level is typically a softening type, in which larger excitation results in more deformation, less equivalent stiffness and more energy dissipation, leading to a high damping system. In such a case, better control of accelerations occurs, reducing the AMR. This will be further discussed in a later section by referring to such hysteresis behavior.

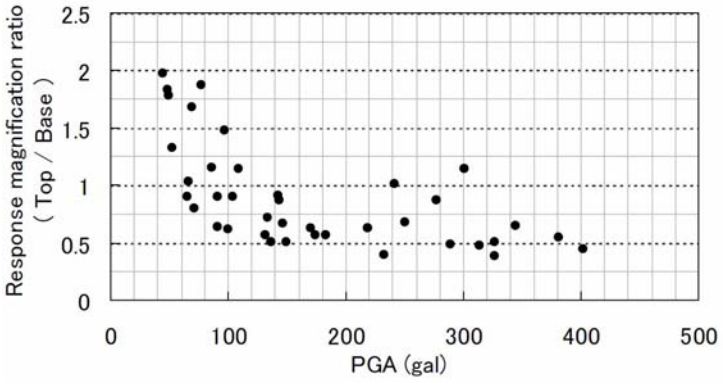

Figure 1. Relationship between acceleration magnification ratio (AMR) and peak ground acceleration (PGA) of base-isolated buildings

In Kanto area where moderate shaking occurred, the responses of low- to mid-rise base-isolated buildings were similar to those observed in the past earthquakes. On the other hand, high-rise base-isolated buildings have shown for the first time the special vibration characteristics which had been expected but not observed until the 2011 East Japan Earthquake. Thus, the subsequent sections will focus on a high-rise base-isolated building to discuss such characteristics.

3. BASE-ISOLATED TALL BUILDING AND MONITORING SYSTEM

3.1. Seismically Isolated Tall Building

Figure 2 illustrates the elevation of the 20-story seismically isolated building, and it is called as "J2-building". Example Building is an office building of Tokyo Institute of Technology located in Yokohama, Kanagawa Prefecture (Kikuchi et al. 2005). Figure 3 shows the plan of the isolation floor of Example Building. The foundation and 1st floor of this building are RC structure. The other floors are hybrid with steel beams and CFT columns.

In the isolated floor of this building, several types of dampers are installed. The 1,200ϕ rubber bearings with conical spring (Figure 4 (a)) are installed in the position (a) as shown in Figure 3. In the position (b), the steel dampers (Figure 4 (b)) are attached, and the 1,100 ϕ rubber bearing with the steel dampers (Figure 4 (c), (d)) are installed in the position (c) and (d), respectively. In the position E, the 1,000kN oil dampers (Figure 4 (e)) are installed.

So called Mega-Braces (□ - 500mm x 160mm x 19 to 32mm) are installed on the both sides of building because the horizontal stiffness is necessary to maintain the seismic isolation effects.

Because this building is very slender shape with the height of 91m and aspect-ratio of 5, tensile force in the rubber bearing becomes a critical design problem. If this tall seismic isolated building suffers a major earthquake, the large up-lift forces may develop at the multi-layer rubber bearings due to the tensile force cause by the large overturning moment. To avoid the large tensile forces, the bearings are enabled to do up-lift in this isolated system (Figure 4 (a)).

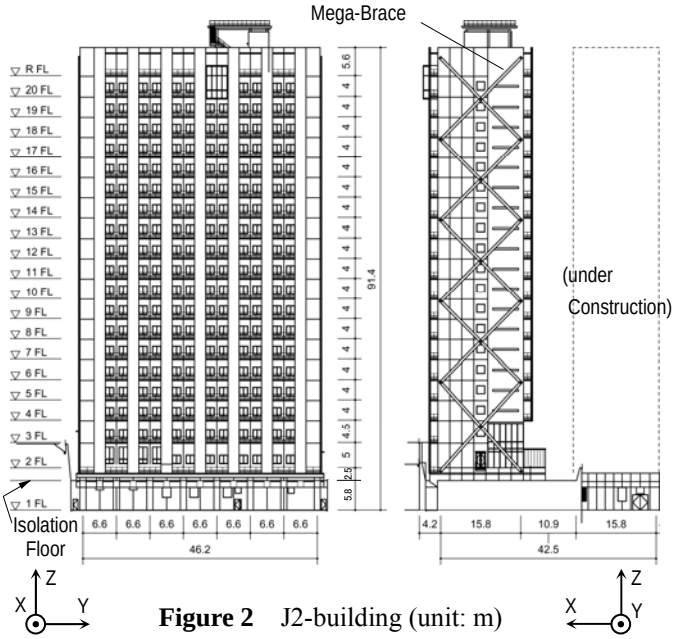

Figure 2 J2-building (unit: m)

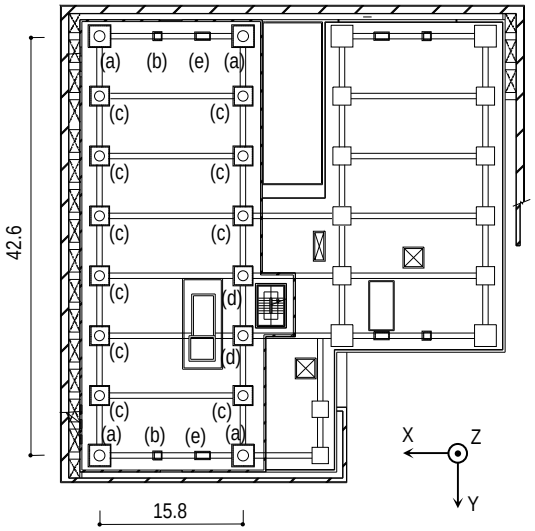

Figure 3 Seismic Isolation Floor (unit: m)

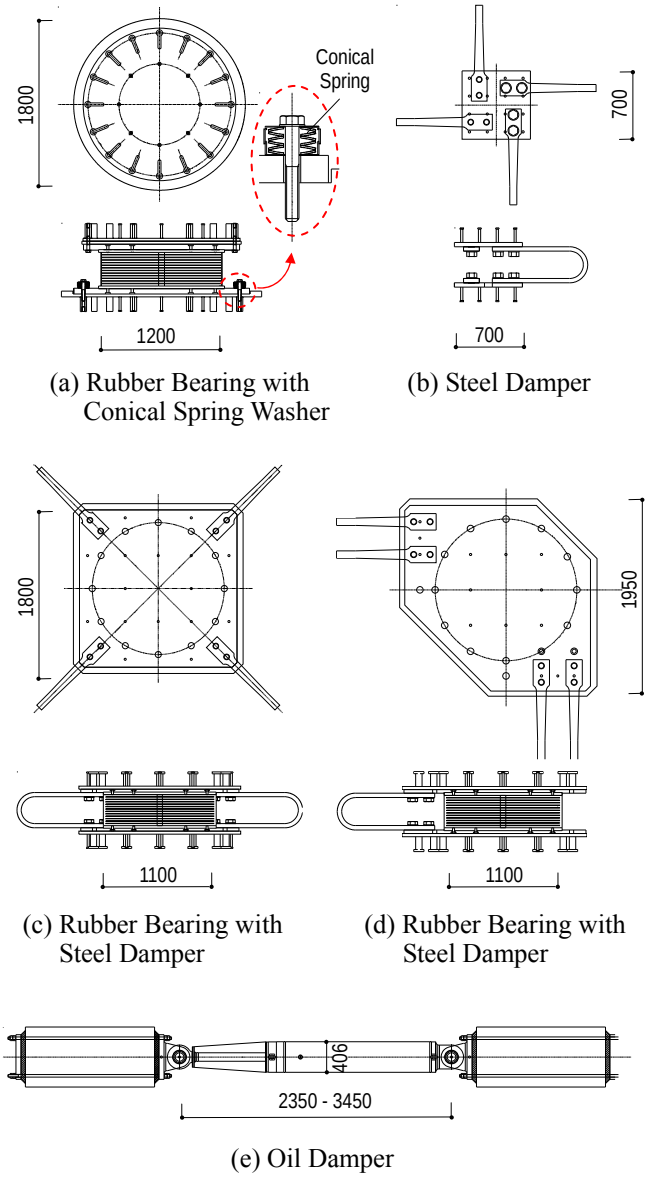

(a) Rubber Bearing with Conical Spring Washer

(b) Steel Damper

(c) Rubber Bearing with Steel Damper

(d) Rubber Bearing with Steel Damper

(e) Oil Damper

Figure 4. Rubber Bearing and Damper (unit: mm)

3.2. Monitoring System

Figure 5 shows the monitoring system and the list of the sensors are indicated in Table 1. In this long-term monitoring system, the accelerometers are placed on the ground surface, 1st, 2nd, 7th, 14th, 20th floor (Sato et al. 2008). This instrument is broad, thus the time history of displacement can be computed by numerical integration. The displacement transducers are installed to measure the displacement of the isolation devices. To measure the large and/or small inter-story displacement in the isolated story level between 1st and 2nd floors, a trace recorder is used in combination with the other measurement devices (see figure 6). The trace recorder is fixed to the steel beam at the bottom of the superstructure while the stainless steel board, on which the behavior of the isolated story is drawn, is fixed to the concrete slab at the top of the substructure. The strain gages are installed at the columns

and the Mega-Braces. Oil damper force and deformation are measured. To measure the up-lift of the isolator as shown in Figure 5(a), the displacement transducers and the video camera are placed.

Output voltage of accelerometers, displacement transducers and strain gages are A/D converted by data loggers installed at each floor, transmitted to data servers through a LAN, and recorded continuously. The clock on data server is set using a GPS signal data on each data logger via the LAN.

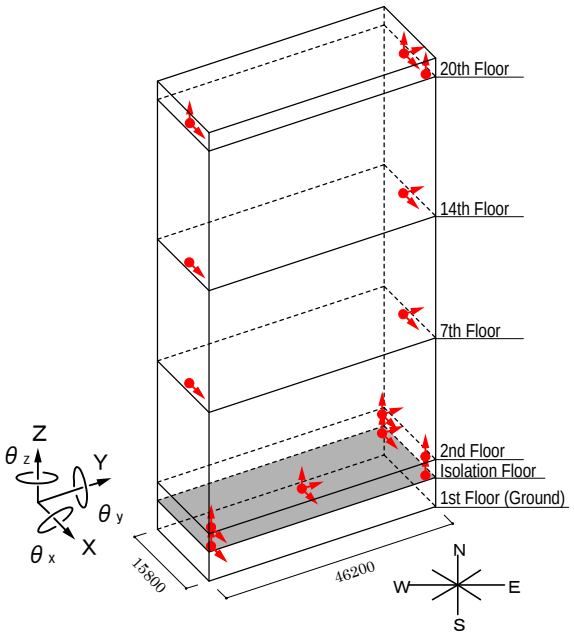

(a) configuration of accelerator

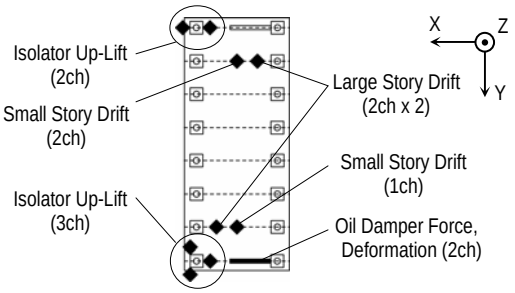

(b) Plan of Isolation Floor

Figure 5 Monitoring System

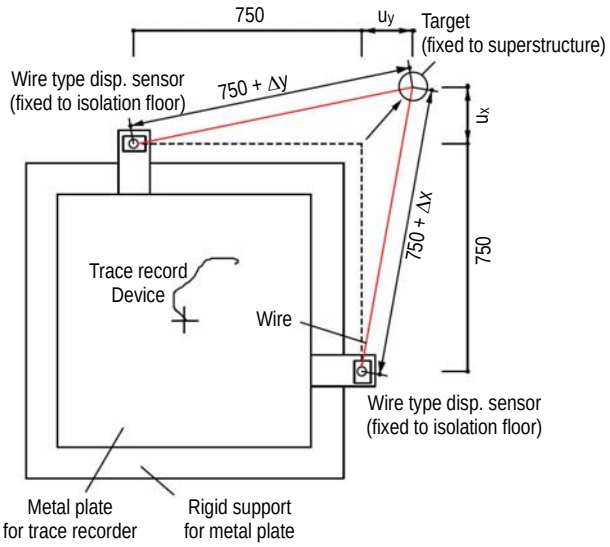

Figure 6. Measurement Device for Large Story Drift in Isolated Story (unit: mm)

Table 1 List of the Sensors

Floor	Item	Capacity	Sensitivity
7, 14, 20F	Acc.	2G	1 μG
	Column, Brace Strain	(Strain Gauge)	1 μstrain
Isolation Floor	Acc.	2G	1μG
	Small Story Drift	±100 mm	0.05 mm
	Large Story Drift	±500 mm	0.5 mm
	Drift Trace	-	-
	Damper Force	(Strain Gauge)	1 μstrain
	Damper Deformation	1000mm	0.5mm
	Isolator Up-Lift	50mm (Video)	0.03mm -
1F	Acc.	2G	1 μG
Ground	Acc.	2G	1 μG

4. RECORDED DATA

The time history of the recorded acceleration at the ground and 20th floor are shown in Figure 7. Peak ground accelerations were 51.4 gal and 67.1 gal in the X- and Y-direction. Peak accelerations at the 20th floor were 87.7 gal and 116.6 gal in the X- and Y-direction. The acceleration magnification ratios (AMR) are 1.7, and they are slightly high. The reason is that the input earthquake motion was lower than the design level. The pseudo-acceleration spectra for the recorded acceleration at the site is shown in Figure 8

Figure 9 show the comparison of the isolated story drift obtained from trace recorders as shown in Figure 6 and from wire type displacement sensors. As shown in Figure 9, these are almost identical, it is consequently indicate that these measurement devices are accurate. As shown in Figure 9, the isolator devices are deformed 69mm and 91mm to X- and Y-direction, and the torsional behavior of isolator level is small since the two results of SW and NE positions are almost same.

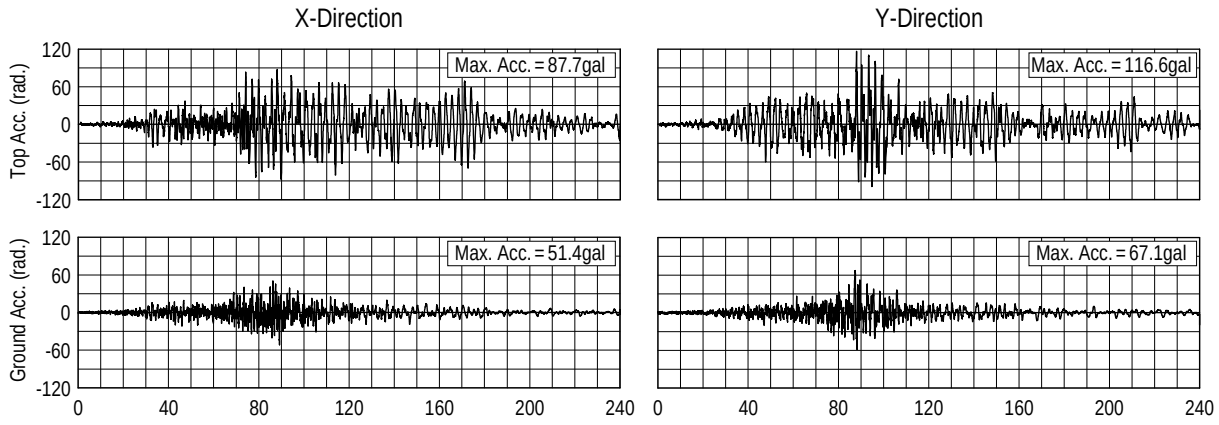

Figure 7. Response spectra for base motions in X and Y directions

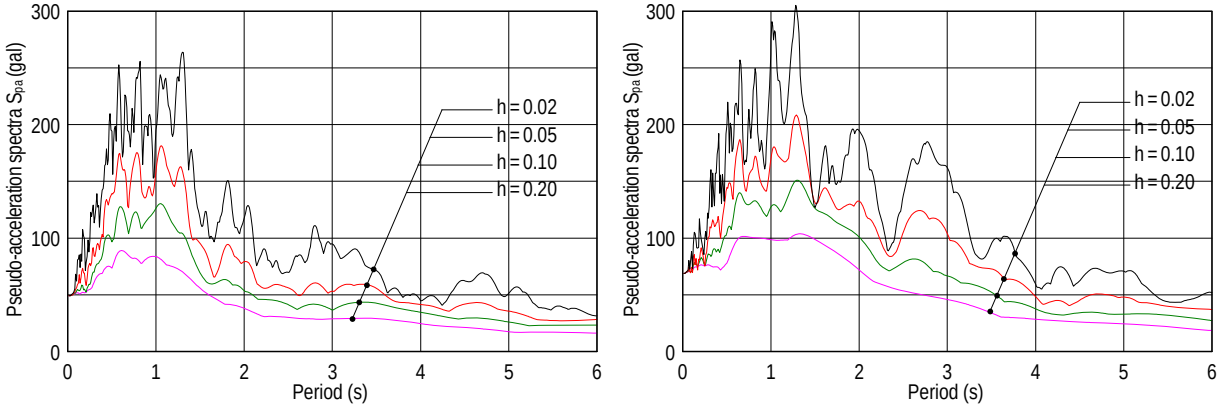

Figure 8. Response spectra for base motions in X and Y directions

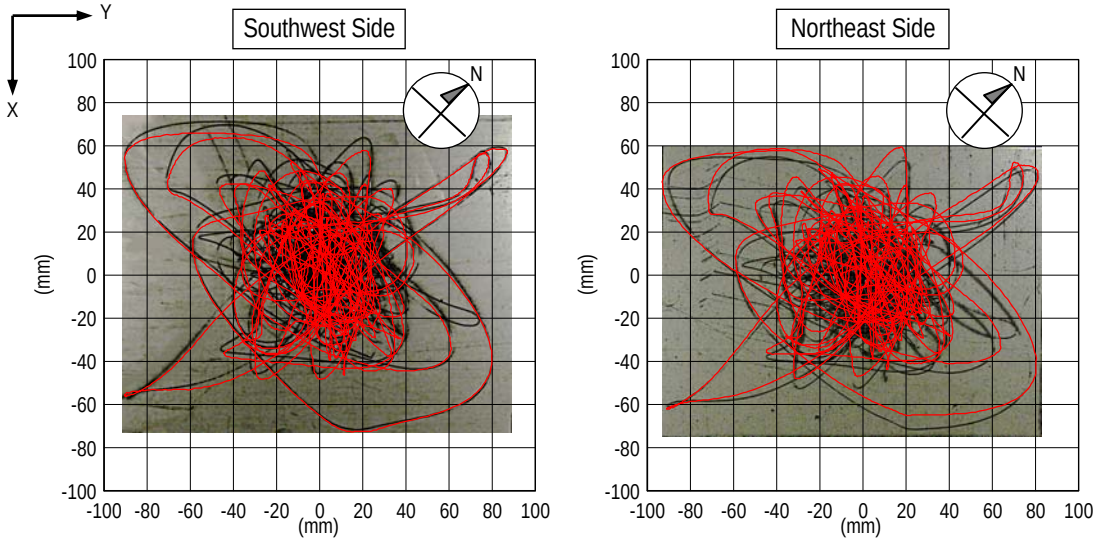

Figure 9. Trace recorder (black lines) vs. wire type displacement sensors (red lines).

5. SYSTEM IDENTIFICATION AND INTERPRETATIONS BY MODAL ANALYSIS

In order to estimate the high-rise building particularly, the two cases, whole structure and superstructure, listed in Table 2 will be discussed in this section. Due to a space constraint, the output of only 20th floor will be indicated in Figures 10 to 12.

Table 2. Acceleration records used as input and output for transfer function, and dynamic properties identified

	Case 1	Case 2
Input Accelerations	Records from 1st floor (ground), below isolator	Records from 2nd floor, above isolator
Output Accelerations	Records from 2nd, 7th, 14th and 20th floors	Records from 7th, 14th and 20th floors
Obtained Dynamic Properties*	Whole building (including isolation system)	Superstructure only

* Dynamic properties mean vibration periods, damping ratios and participation vectors from the 1st mode to 3rd mode

5.1. System Identification

Natural frequencies, damping ratios and modal participation vectors are computed by curve-fitting the idealized transfer function assuming steady-state response to the empirical transfer function estimated from acceleration data. The amplitude of the empirical transfer function is ratio of Fourier spectrum amplitude spectra at the top and base (or 2nd floor) of the building. Moreover, the phase angle of the empirical transfer function is the ratio between real and imaginary parts of the Fourier spectra. Example of transfer function amplitude and phase angle, along with the fitted idealized curve, is shown below in Figure 10. 1st mode vibration periods and damping ratio of are estimated as listed in table 3

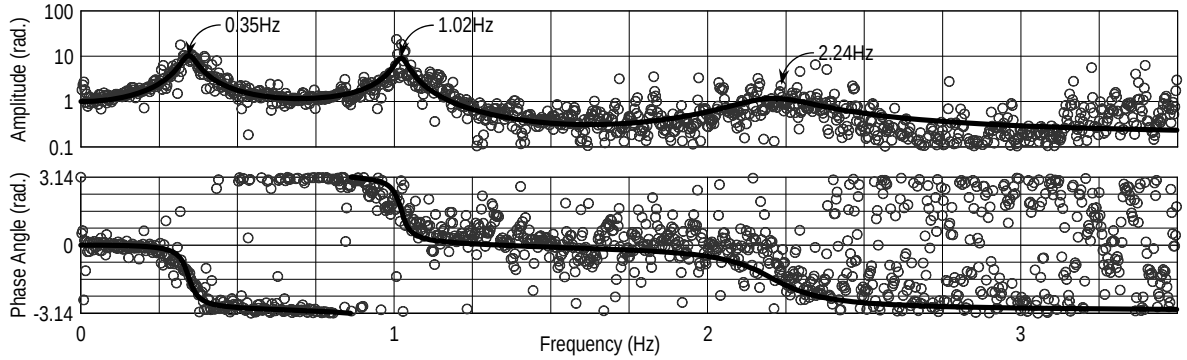

(a) Case 1: derived from records at 20th floor and 1st floor (below isolator)

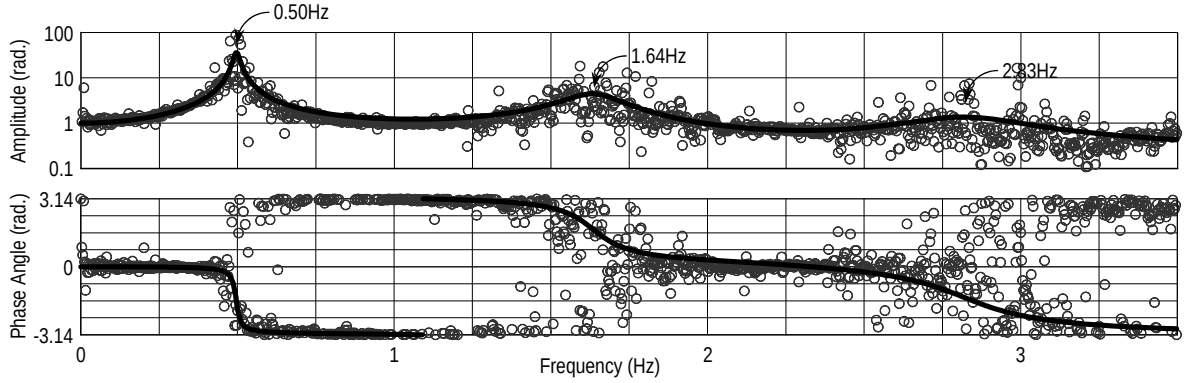

(b) Case 2: derived from records at 20th floor and 2nd floor (above isolator)

Figure 10. Example of transfer function and curve-fitting in X-direction

Table 3. 1st mode vibration periods and damping ratio

	X-direction		Y-direction	
	Period (s)	Damping ratio	Period (s)	Damping ratio
Base-isolated case (total building)	2.92	0.070	2.98	0.105
Seismic resitant case (only superstracture)	2.01	0.021	2.15	0.046

5.2. Modal Analysis

Dynamic analysis by modal superposition was conducted using the first three estimated modal frequencies, damping ratios and modal participation vectors. A comparison of top-level displacement and acceleration from modal analysis and recorded response in both base-isolated case and seismic resistant case are shown in Figure 11, respectively. The displacement was obtained from the acceleration record by double integration together with hi-pass filtering in frequency domain. The cut-off frequency is typically 0.05 Hz. The modal analysis results are reasonably close to those observed in the earthquake, validating the results of the system identification method and measurement system.

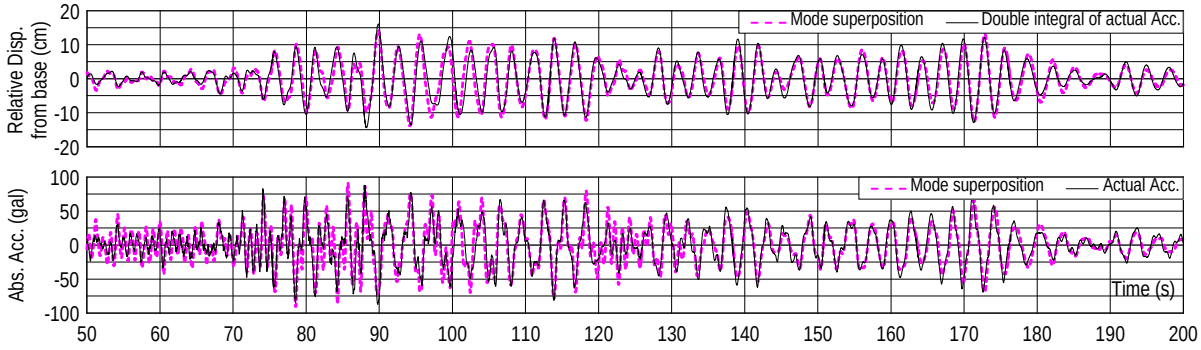

(a) Case 1: Analysis of whole structure (isolation system included), using 1st floor accelerations as input.

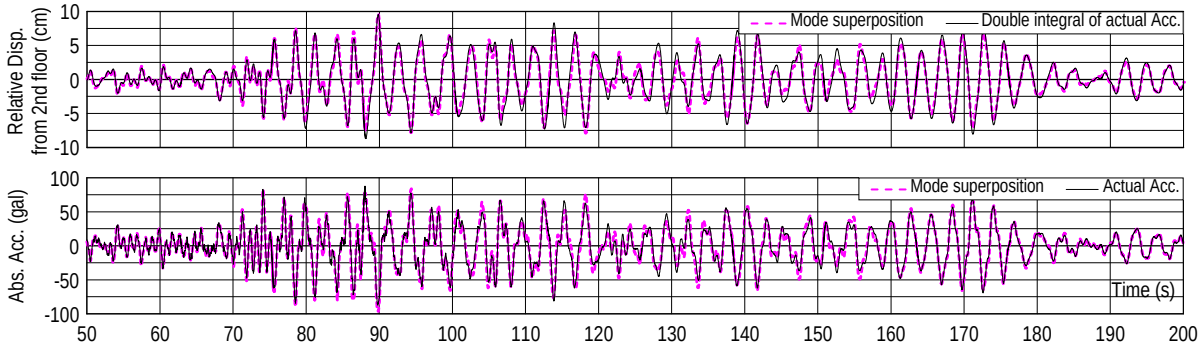

(b) Case 2: Analysis of superstructure only, using 2nd floor accelerations as input.

Figure 11. Comparison of top-level behavior between recorded data and modal analysis using identified modal frequencies and damping ratios in X-direction

5.3. Effect of Base-Isolation System

The case that there is no base-isolation system in this building is discussed. Assuming the base-isolator as rigid, the superstructure model obtained from Section 5.1 is subjected to the acceleration record of base level.

Comparison of base-isolated case and seismic-resistant case is shown in figure 12. Although the difference of displacement between the seismic-resistant case and the base-isolated case is not so large, the acceleration of the seismic-resistant case is twice as much as that of the base-isolated case. Therefore the base-isolation system has functioned effectively.

6. NONLINEAR BEHAVIOR DUE TO STEEL DAMPER YIELDING

Using acceleration data and the estimated inertial mass of the structure, hysteretic response of the isolation level was also computed, as shown in Figure 13. The absolute accelerations of each floor

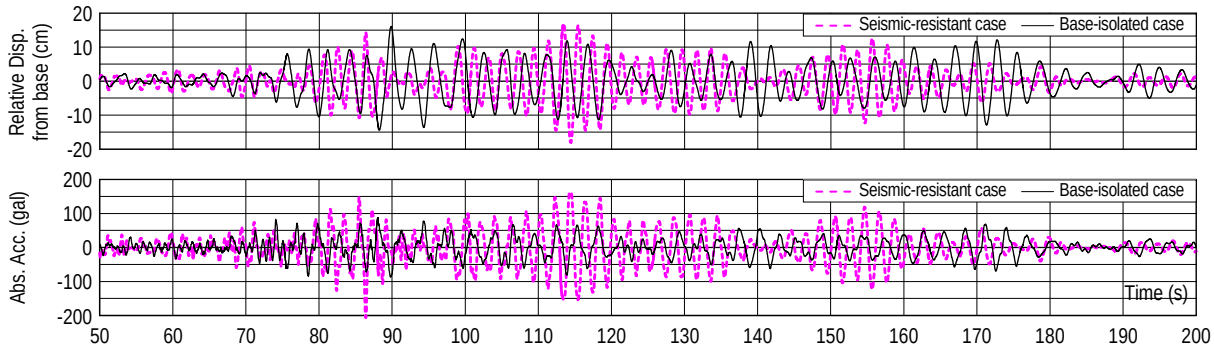

Figure 12. Comparison of base-isolated case and seismic-resistant case by modal analysis (Top of X-direction)

were estimated by the acceleration records of 2F, 7F, 14F, 20F and linear interpolation. The relative displacements above and below the isolation plane were estimated by the difference of absolute displacement which is computed by double integration of the acceleration records. The hysteresis is shown for three distinct phases of excitation, clearly showing the linear and bilinear nature of the response caused by the steel damper. The envelope curves are in excellent agreement with the design curves, therefore the steel damper has functioned as previously supposed. Although the linear stiffness before large deformation is same as design curve of steel damper (see Figures 13(a) and (d)), the linear stiffness after large deformation declines slightly (see Figures 13(c) and (f)).

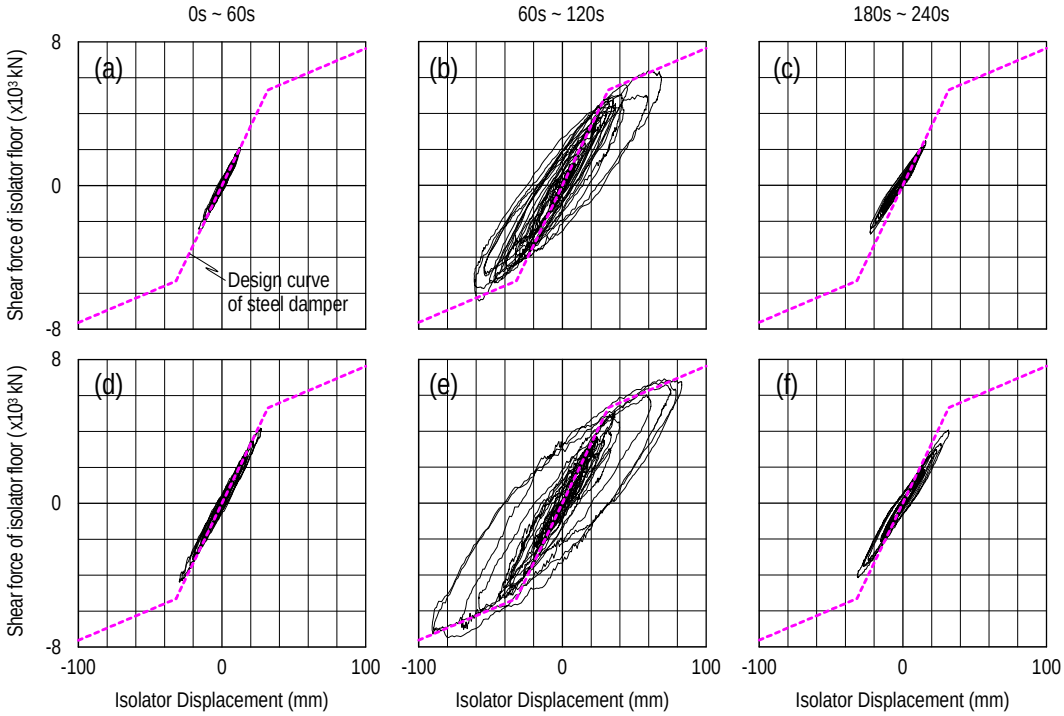

Figure 13. Hysteresis of isolator floor (a) ~ (c) : X-direction, (d) ~ (f) : Y-direction

Figure 14(a) shows the relative displacement above and below the isolation plane, and Figures 14(b) and (c) show the results of the autoregressive with exogenous inputs (ARX) method (Isermann and Münchhof, 2011) using the accelerations of the ground and 20th floor. The dynamic properties vary over time, depending on the level of displacement in Figure 14(a). Therefore larger isolation effect could be expected against the larger earthquake motion. During the maximum displacement excursions, between 80 and 110 seconds, the building frequencies including isolation are declining. The estimated first mode damping ratio also shows significant variation over the duration, and appears to be between 0.07 and 0.15 during significant shaking. These changes of the dynamic properties during shaking are due to the bilinear characteristics of the isolation system. The frequencies

obtained from ARX are lower than the values obtained from curve fitting (Section 5.1). The reason is that whole data is used in the case of curve fitting, but divided data is used in the case of ARX.

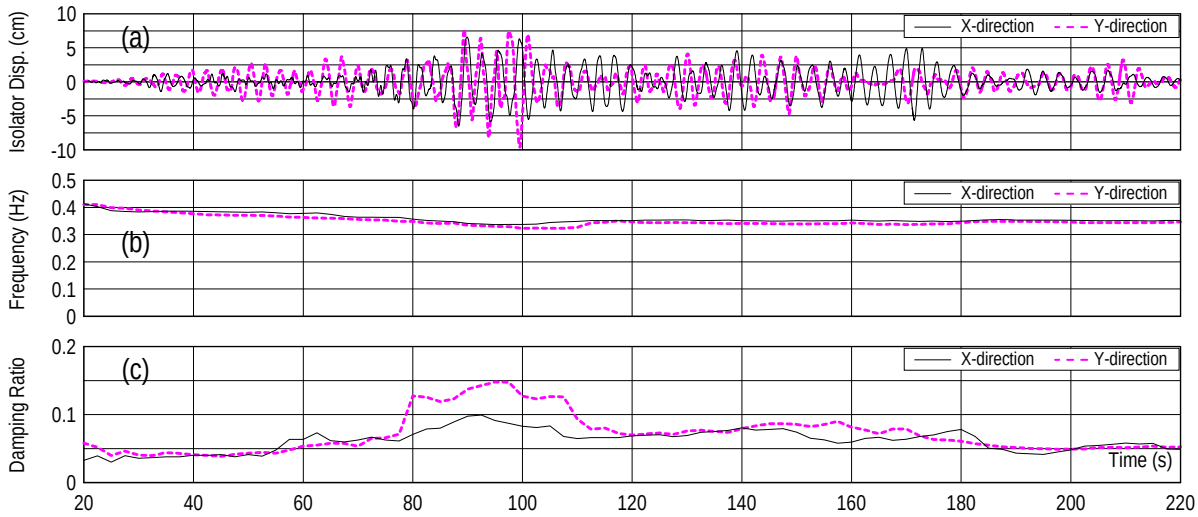

Figure 14. Variation of dynamic properties
(a) isolation plane displacements, (b) first mode natural frequencies and (c) first mode damping ratios

7. EFFECTS OF SHAKING LEVEL ON DYNAMIC PROPERTIES AND RESPONSES

The vibration periods and damping ratios are estimated by the curve fitting method (Section 5.1) in 5 times,(a) microtremor measurement, (b) March 9 earthquake, (c) March 11 East Japan Earthquake, (d) March 11 afterquake and (e) microtremor measurement. Earthquake motions (b) and (d) are almost half level of Earthquake motion (c) and the results are shown in Figure 15. The larger earthquake motions become, the more base-isolation effect become, high damping and long period. Therefore larger isolation effect could be expected against the larger earthquake motion.

Although the acceleration magnification ratios is about 1.7 in main earthquake (see Figure 16), the value went up to about 3.1 against relatively weak earthquake motion. It seems to be caused by, in addition to above effect, the deformation mode of high-rise base-isolation building. Therefore, in the case of weak earthquake motion, the equivalent stiffness of the isolation plane is relatively high and the building behaves like seismic-resistant structure. This behavior should be discussed in the near future.

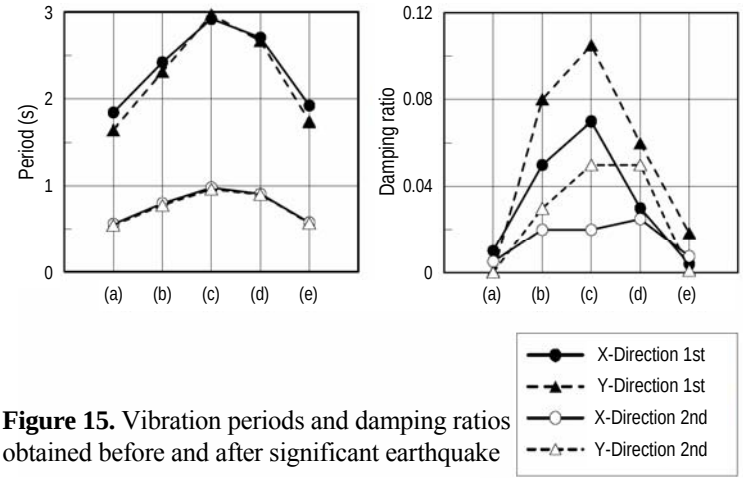

Figure 15. Vibration periods and damping ratios obtained before and after significant earthquake

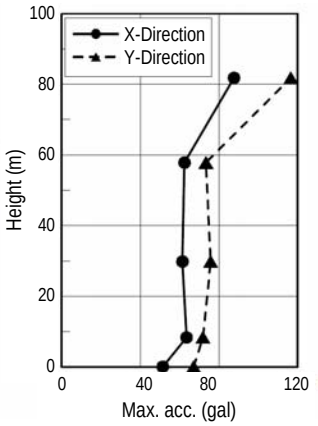

Figure 16. Peak acceleration

8. CONCLUSIONS

Dynamic properties of a high-rise base-isolated building were discussed by using records which were obtained on March 11, 2011. Major findings are:

- The maximum displacement 23cm of the isolation system was recorded in this earthquake. In spite of long distance from the earthquake center, the value was the largest displacement since final completion.
- In the two cases (total structure and only superstructure), natural frequencies, damping ratios and modal participation vectors were estimated by curve-fitting of transfer function. Moreover the accuracy of the estimated values was confirmed by comparison between recorded data and dynamic analysis of modal superposition.
- It was confirmed that the base-isolation system has functioned effectively. In particular, the isolation system was supposed to reduce acceleration response by half.
- The steel dampers are mainly used in isolation floor as energy dissipation device, therefore the hysteresis of isolation floor clearly showed the bilinear nature of the response. Larger isolation effect could be expected against the larger earthquake motion.

REFERENCES

JSSI (2012), Japan Society of Seismic Isolation, Report of Response-Controlled Buildings Investigation Committee, January 26, 2012

Kasai, K., Mita, A., Kitamura, H., Matsuda, K., Morgan, T., and Taylor A., Performance of Seismic Protection Technologies During the 2011 East Japan Earthquake, Earthquake Spectra, special issue (in Review)

Kikuchi, T., Fujimori, S., Takeuchi, T., and Wada, A. (2005), “Design of High Rise Seismic Isolated Steel Building with Mega-Bracing System, Journal of Technology and Design, Architectural Institute of Japan, No20, 217-222, Dec. (in Japanese)

Sato, D., Ooki, Y., Morikawa, H., Yamada, S., Sa-kata, H., Yamanaka, H., Kasai, K., Wada, A. and Kitamura, H. (2008), “Evaluation of Seismically Isolated Tall Building Based on Long-Term Monitoring, Proceedings of The 14th World Conference on Earthquake Engineering (14th WCEE), Beijing, China

Isermann, R. and Münchhoff, M. (2011) Identification of Dynamic Systems: An Introduction with Applications, Springer, New York.